Research on
Engineering
Structures & Materials
journal homepage: http://jresm.org

RESEARCH
GROUP

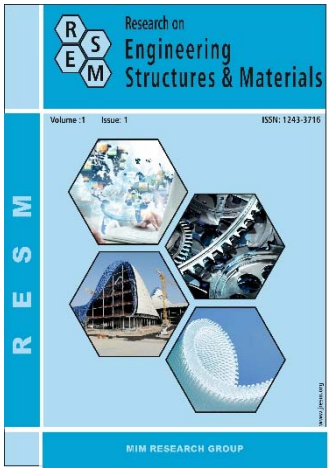

Effects of Permeable Cylinders on Wake Region

Bengi Gözmen*, Hüseyin Akıllı

Online Publication Date: 06 July 2015
URL: http://www.jresm.org/archive/resm2015.09en0529
DOI: http://dx.doi.org/10.17515/resm2015.09en0529

Journal Abbreviation: *Res. Eng. Struct. Mat.*

To cite this article
Gozmen B, Akilli H. Effects of permeable cylinders on wake region. *Res. Eng. Struct. Mat*., 2015; 2: 109-120.

Research on
Engineering
Structures & Materials
journal homepage: http://jresm.org

RESEARCH
GROUP

Research Article

Effects of Permeable Cylinders on Wake Region

Bengi Gözmen*[1], Hüseyin Akıllı[2]

1 Mersin University, Department of Mechanical Engineering, TURKEY
2 Cukurova University, Department of Physics, TURKEY

Article Info

Article history:
Received 29 May 2015
Revised 3 July 2015
Accepted 13 July 2015

Keywords:

Circular cylinder
Vortex shedding
PIV

Abstract

This paper investigates the effects of permeable cylinder on vortex shedding downstream of the permeable cylinder in deep water flow by PIV technique. In order to reveal the effect of porosity β on the vortex shedding, the permeable cylinder having four different porosities (β = 0.4, 0.5, 0.6 and 0.7) with a diameter of 45 mm have been used. During the experiments, the free-stream velocity is U∞= 156 mm/s, which corresponds to the Reynolds number of Re=5000 based on the solid cylinder diameter. The experiments show that the permeable cylinder is effective on the suppression of vortex shedding in the wake region for all porosities and in terms of the inner cylinder-outer permeable cylinder arrangement, it is understood that the inner-outer cylinder arrangement having the diameter ratio of D/d=1.5 is not effective on the attenuation of vortex shedding downstream of the inner cylinder-outer cylinder arrangement as expected. The inner and outer permeable cylinders behave like an impermeable cylinder having the diameter of D=45 mm for the porosities of β = 0.4, 0.5 and 0.6. The suppression of the large scale vortices is weak. On the other hand, for the porosity β = 0.7, the peak value of Reynolds shear stress drops to 0.0368 which is less than that of the bare cylinder. The reduction of $< u'v' >$ is approximately 10%.

1. Introduction

The phenomenon of vortex shedding from bluff bodies has been a challenging interesting problem in fluid dynamics and engineering. Vortex shedding from a bluff body usually causes to serious structural vibrations, acoustic noise, resonance and substantial increases in the mean drag and lift fluctions [1]. Though there have been numerous studies on the vortex shedding, the mechanism of vortex shedding has not yet been clearly understood. Significant efforts have been made to mitigate the negative effects of vortex shedding and various methods on the suppression of vortex shedding have been developed. These methods can be categorized into two main techniques: active and passive controls. Active control methods are based on applying some sorts of external energy into the flow field while the passive control techniques control the vortex shedding by modifying the shape of the bluff body or by attaching additional devices in the flow. Rotational oscillaratory [14], suction and blowing [15, 16], syntetic jet [17], piezo actuators [18] are examples of

*Corresponding author: bengigozmen@gmail.com
DOI: http://dx.doi.org/10.17515/resm2015.09en0529
Res. Eng. Struct. Mat. Vol.1 Iss.2 (2015) 109-120

active control methods in order to suppress the unsteady flow structure of bluff body. On the other hand, splitter plates, small rods, roughness elements, helical wires, porous and permeable materials as passive control techniques are applied to attenuate effects of vortex shedding. Among these control techniques, an external small element placed downstream of the main body, was studied by Strykowki and Sreenivasan [2]. They set a significantly smaller circular cylinder parallel to the main circular cylinder. Vortex shedding from body sides of the main body can be suppressed at Reynolds numbers smaller than 100. Another researcher group, Lee et.al. [3] used the small control rod to control the vortex shedding behind the cylinder. They revealed that the drag coefficient and wake structure changed significantly depending on pitch distance L between the main cylinder and control rod. Lim and Lee [4] investigated the wake region behind circular cylinders fitted with 0-rings. They observed that the vortex formation region behind the cylinder elongated and the width of the wake was decreased.

One of the successful methods in the passive control methods is the splitter plate to control the vortex shedding around the bodies and there are many studies on the splitter plate placed downstream of the cylinders in the literature. Kwon and Choi [5] tried to the control of laminar vortex shedding downstream of a circular cylinder using splitter plates. They revealed that the vortex shedding downstream of a circular cylinder completely disappeared when the length of the splitter plate was longer than a critical length, and this critical length was proportional to the Reynolds number. Ozono's study [6] showed that the vortex shedding could be suppressed even when the splitter plates were arranged asymmetrically downstream of the cylinder and the length of splitter plate did not have much effect on the flow structure in the case of asymmetric arrangement. The thickness effect of splitter plate on the suppression of vortex shedding was investigated by Akilli et al. [7]. They revealed that the change in the splitter plate thicknesses did not have any considerable effect on the flow structure. Gozmen et.al.[8] researched the effect of the splitter plates having different heights and lengths located in the wake region of the circular cylinder in shallow water. Shukla et. al. [9] experimetally investigated the effects of the flexiable splitter plate on the vortex structure. They found that the splitter plate length (L) and the flow speed (U), the flexural rigidity (EI) of the splitter plate were important parameters to control the flow.

Another method of passive control technique is the usage of porous and permeable devices in order to control the flow around bluff bodies. Sobera et al. [13] investigated flow structure at subcritical Reynolds number (Re=3900) around a circular cylinder surrounded by porous layer. They found that the flow in the space between the porous layer and the solid cylinder was laminar and periodic. Moreover, the frequency of flow was locked to the Strouhal frequency of vortex shedding in wake region. Bruneau and Mortazavi [10] focused on the control of the flow around a fixed cylinder using a porous layer between the obstacle and the fluid. They showed that the porous layer reduced the shear effects in the boundary layer and change the structure of vortex shedding. Bhattacharrya et al. [11] studied on flow structure around and through a porous cylinder. They revealed that the flow field was steady for the range of Reynolds number ($1 \leq Re \leq 40$) and the drag force decreased monotonically while the Reynolds number was increasing and the Da was decreasing. Ozkan et al. [20] carried out an experimental study on the control of flow around a cylinder surrounded by a permeable cylinder in shallow water. They proved that both porosity and outer cylinder diameters had significant effects on the attenuation of vortex shedding downstream of the circular cylinder in shallow water. The peak values of turbulent statistics, like turbulent kinetic energy (TKE) and Reynolds stresses were decreased significantly by the permeable cylinder. Pinar et al. [21] studied on the control flow around the perforated cylinders having the porosities in the range of $0.1 \leq \beta \leq 0.8$ with an increment of 0.1. They depicted that the fluctuations were reduced

dramatically in the wake region by the use of a perforated cylinders and the interval of $0.4 \leq \beta \leq 0.8$ for the porosity could be advised for effective suppression of KarmanVortex Street. Bovand et al. [22] performed a numerical study on flow around a porous circular cylinder in the existence of a cross radial magnetic field. This study was different from the papers on the porous devices mentioned above in terms of the used method. They created a magnetic field and placed a porous circular cylinder in this field. They showed that the Stuart number for disappearance the re-circulating wake increased with increased Reynolds number for both porous and solid cylinders. Gozmen and Akilli [12] studied on the control of the flow around a circular cylinder surrounded by outer permeable cylinder in deep water. The results of this work indicated that both the porosity and the diameter ratio D/d were the parameters which played important role on the suppression of vortex shedding downstream of the cylinder arrangement. The outer permeable cylinder reduced the wake instabilities and vortex shedding around the cylinder arrangement depending on the porosity and the diameter ratio.

The objective of this paper is to investigate experimentally the effects of the permeable cylinders of 45 mm diameter having different porosities on the vortex shedding downstream of the solid cylinder in deep water. Permeable cylinders used during the experiments are constructed of a chrome-nickel wire mesh as noncorrosive material since the main aim of this study is to control the vortex shedding around or downstream of the cylindrical structures under water like bridge piers. To obtain velocity field information in the wake, the particle image velocimetry (PIV) technique was used.

2. Materials and Method

Experiments were carried out in a water channel, having dimensions of 8,000 mm x 1,000 mm x 750 mm, located at Çukurova University, Fluid Mechanics Laboratory of Mechanical Engineering Department, Turkey.

Experiments were performed in two steps: dye visualization experiments and PIV. At the first step, flow visualization experiments were carried out using Rhodamine type dye that shines under the continuous laser beam in the desired flow field. Visualization of the experimental results was captured with a high speed SONY 80X handycam type digital video recorder. In the second step, the PIV method was used as the investigation tool to calculate instantaneous and mean velocity field behind a circular cylinder in order to understand the effect of the permeable cylinders on the vortex shedding in wake region as the study of Gozmen and Akilli [12]. Figure 1 shows a side-view of the experimental system. The flow structures of a circular cylinder with a diameter of d=30 mm made from the transparent plexiglass material, permeable cylinder made of a chrome-nickel wire mesh and the inner-outer cylinder arrangement composed of the outer permeable cylinder concentrically placed around the inner cylinder were researched. In this study, porosity was defined as the ratio of gap area on the body to the whole body surface area (Fig. 2.) And the porosities of the permeable cylinder were selected as β= 0.4, 0.5, 0.6 and 0.7. The ratio of permeable cylinder diameter to inner cylinder diameter, D/d was selected as 1.5, i.e. the inner cylinder diameter was d=30 mm where the outer cylinder diameter is D=45mm and the permeable cylinder was concentrically located around the inner cylinder. All experiments were carried out above a platform and the cylinder was placed at 1750 mm from the leading edge of the platform in order to obtain fully developed boundary layer. Total depth of the water channel was adjusted to 560 mm. The water height between the base of platform and the free surface (h_w) was set at 340 mm The flow measurement was performed at the mid-depth of the water between the base of platform and the free surface (h_L). The free-stream velocity was U= 156 mm/s, which corresponds to the Reynolds number of Re=5000 based on the solid cylinder diameter. This velocity was adjusted by a centrifugal pump with a speed control unit.

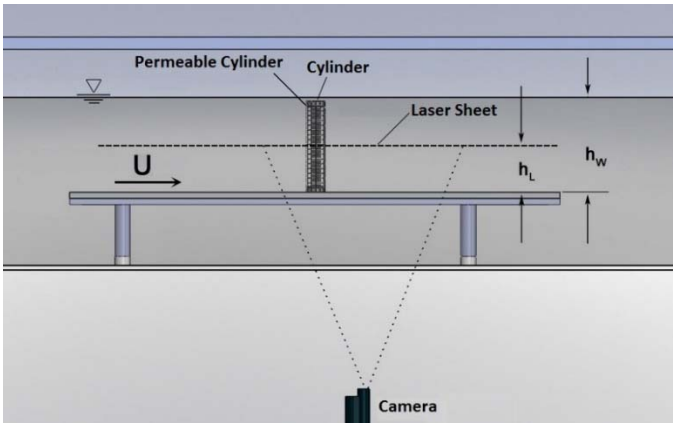

Fig. 1. Side view of the experimental system

Quantative flow images were acquired and processed by Dantec Dynamic PIV system and Flow Manager Software. A pair of double-pulsed Nd:YAG laser units each having a maximum energy output of 120mJ at 532nm wave length illuminated the measurement field. The thickness of the laser sheet illuminating the measurement plane was approximately 2 mm. An 8 bit cross correlation CCD camera with a resolution of 1600x1200 pixels, equipped with a Nikon AF micro 60 f/2.8D lens captured the flow fields. The camera and laser pulses were triggered with correct sequence and timing using a synchronizer. In the image processing, 32x32 pixels rectangular effective interrogation windows were used. During the interrogation process, an overlap of 50 % was employed in order to satisfy Nyguist criterion. A total of 3844 (62x62) velocity vectors were obtained for an instantaneous velocity field at a rate of 15 frames per second. For all experiments, two views one after the other were taken and every field of view was 200x200 mm^2. The water was seeded by silver-coated hollow glass spheres of 12 μm mean diameter and the density of the particles was 1100 kg/m^3. The Stokes Number of the particles which provides a measure of the ability of particles to track the flow field was calculated about $1.83x10^{-4}$ [12]. This meant that the particles in these experiments followed the streamlines completely. In each experiment, 350 instantaneous images were captured, recorded and stored so as to obtain averaged-velocity vectors and other statistical properties of the flow field. In current study, the uncertainty in velocity relative to the depth-averaged velocity was about 2%.

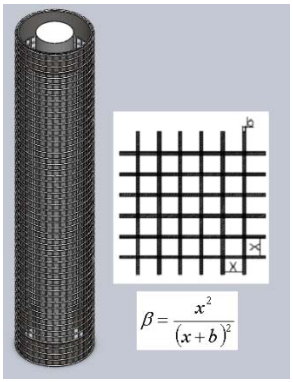

Fig. 2. Schematic placement of inner cylinder and outer permeable cylinder

3. Results

This section presents dye visualization and PIV results of the bare cylinder, permeable cylinder and the flow structure of inner-outer permeable cylinder arrangement.

3.1. Dye Visualization

Figure 3 shows dye images obtained from the dye visualization. It is understood that the well-known Karman Vortex Street occurs downstream of the bare cylinder. For the permeable cylinder having the porosity of β = 0.4, low frequency Karman Vortex Street in comparison with that of the bare cylinder forms downstream of the permeable cylinder. On the other hand, for the porosity of β = 0.7 Kelvin-Helmholtz instabilities start to play an important role in the shear layers instead of Karman Vortex Street. Beside this, the wake region contracts in the cross-stream direction since the open area on the surface of the permeable cylinder is too large to prevent the flow and the flow rapidly moves streamwise direction without diffusing into the permeable cylinder. At the last row, the quantitative dye images of the inner cylinder- outer permeable cylinder arrangement are shown. For the cylinder arrangement having the permeable cylinder with the porosity of β = 0.4, well-known Karman Vortex Street occurs downstream of the cylinders as the bare cylinder case since the outer permeable cylinder behaves like an impermeable cylinder with the diameter of 45 mm. For the porosity of β = 0.7, the flow structure shows a bit difference from the bare cylinder case. The flow in the wake region forms like "S" shape as a result of low frequency vortex shedding. The occurrence of vortex shedding moves away from the base of the outer permeable cylinder.

3.2. PIV Results

3.2.1. Bare Cylinder Case

To explain the flow structure downstream of the bare cylinder, normalized Reynolds stress contours, dimensionless turbulent kinetic energy contours and the streamwise velocity contours, respectively, are indicated in Figure 4. The Reynolds stresses directly control the dynamics of the vortical structures. And TKE, which is directly related to the dynamics of the vortices and usually used as the measurement of the turbulence mixing [23] can be calculated with the following expression;

$$TKE = \frac{3}{4}[\langle u'u' \rangle + \langle v'v' \rangle] \quad (1)$$

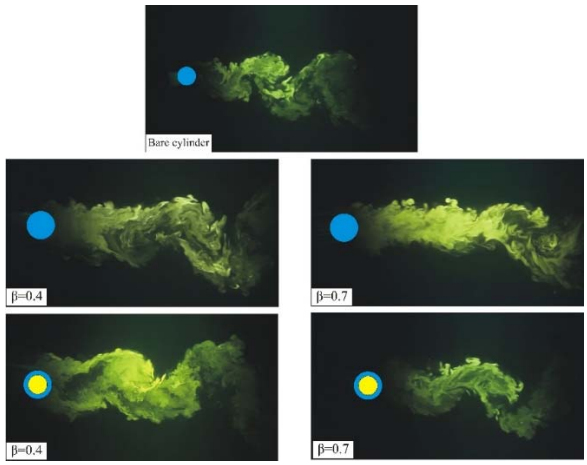

Fig. 3. Instantaneous dye images

Both minimum and incremental values of the contours of of Reynolds shear stress were taken ±0.002 and 0.002. As the solid lines present the positive (counter-clockwise) Reynolds shear stresses, the dashed lines show the negative (clockwise) Reynolds shear stresses. This figure demostrates that both the positive and negative Reynolds shear stress contours extend symmetrically along the centerline of the cylinder. The contours of Reynolds shear stress $< u'v' >$ consist of both small-scale clusters located in the vicinity of the base of the cylinder and large scale clusters located just downstream of the small-scale clusters due to the the flow entrainment into the wake region. The peak value of Reynolds shear stress is approximately 0.0405 and it occurs in the first field of view. The turbulent kinetic energy (TKE) contours presented in the second row shows that the location of peak value of TKE coincides with the location of peak value of the Reynolds shear stress and the peak value of turbulent kinetic energy is 0.138. After the location of the peak value, the turbulent kinetic energy contours dissipate gradually in the flow direction. The last row presents the contours of time-averaged streamwise velocity in this figure. The minimum and incremental values of the streamwise velocity contours were selected as ± 5 and 5, respectively. The substantial region of reverse flow is clearly seen in this figure as a result of momentum transfer from the free-stream flow into the wake region. The location of negative velocity contours is approximately 1d from the base of the cylinder and the peak value of negative streamwise velocity is nearly 0.121.

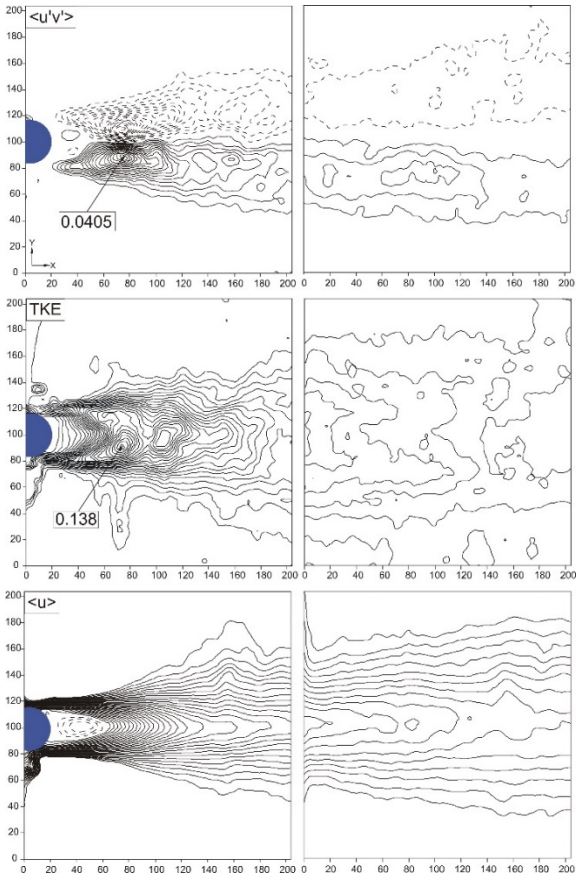

Fig. 4. The flow structure downstream of bare cylinder case (Both minimum and incremental values of the contours of TKE were taken as 0.005in this figure)

3.2.2. Permeable Cylinder Case

The flow characteristics of permeable cylinder having the diameter of D = 45 mm for the porosity values β of 0.4, 0.5, 0.6 and 0.7 are given in Figure 5. This figure demonstrates the contours of the normalized Reynolds shear stress $<u'v'>$ and the time-averaged streamwise velocity. The minimum and incremental values of Reynolds shear stress were selected as ± 0.001 and 0.001, respectively. Furthermore, for the streamwise velocity contours, the minimum and incremental values were taken as ± 5 and 5, respectively. As all cases in this study, for both the contours of Reynolds shear stress and the time-averaged streamwise velocity, the solid lines and the dashed lines present positive (counter-clockwise) and negative contours, respectively. This figure shows that a decrease in Reynolds stress which implies drag reduction in the wake region is obtained by permeable cylinders. The peak values of Reynolds shear stresses for porosity values of β = 0.4 and 0.5 is approximately 60 % of that of the bare cylinder. For the porosity of β = 0.70, the peak value of drops to 0.0053 nearly 13 % of that of the bare cylinder. This means that Reynolds shear stress substantially decreases with increasing the porosity as a consequence of enlarged open area on the surface of the permeable cylinder. The contours of streamwise velocity for the porosity range of 0.4 ≤ β ≤ 0.7 are illustrated at the right side of Figure 5. For all porosity values, the reverse flow does not form in the fields of view while the peak value of negative streamwise velocity is about 0.121 for the bare cylinder case.

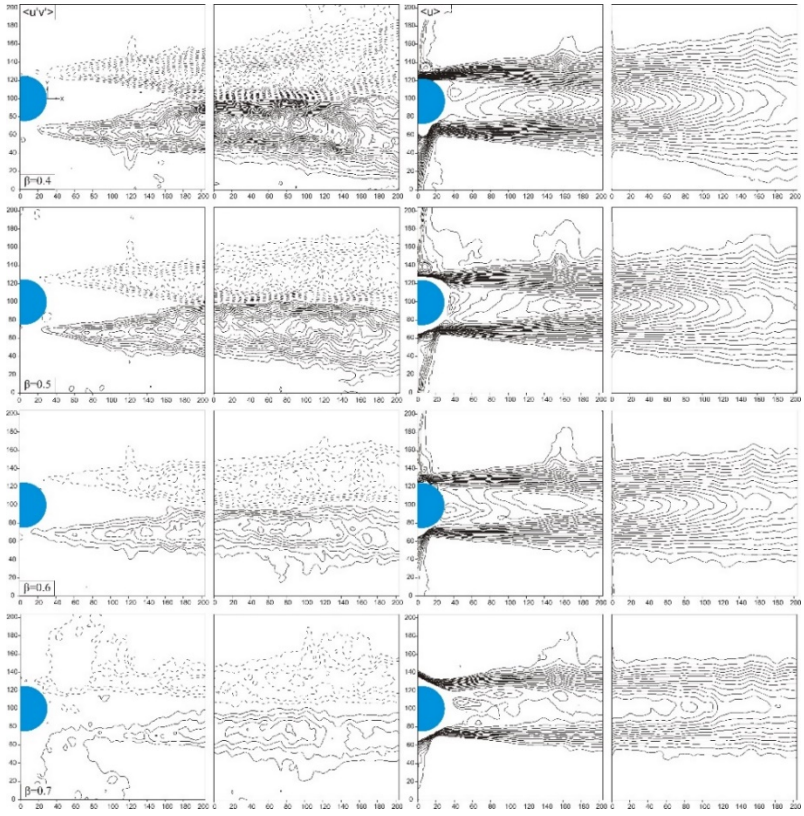

Fig. 5. Contours of normalized Reynolds shear stress and time-averaged streamwise velocity downstream of the permeable cylinder for all porosity values β of the diameter D=45 mm

3.2.3. Inner Cylinder- Outer Permeable Cylinder Arrangement

To suppress the vortex shedding downstream of the circular cylinder, permeable outer cylinder having the diameter of D=45 mm was concentrically located around the inner cylinder. Four different values of porosity were used such as β = 0.4, 0.5, 0.6 and 0.7. In order to elucidate the effect of porosity for the diameter ratio of D/d=1.5, the contours of normalized Reynolds shear stress and streamwise velocity component obtained from the PIV experiments are presented in Figure 6. This figure depicts that the outer permeable cylinder cannot suppress concentration of downstream of the inner cylinder except the porosity of β = 0.7. For the porosities of β = 0.4, 0.5 and 0.6, the wake region downstream of the inner-outer cylinder arrangement extends along the streamwise direction compared to the bare cylinder wake. But the peak values of Reynolds shear stress increase to 0.0458, 0.472 and 0.0468, respectively. On the other hand, for the porosity β = 0.7, the peak value of Reynolds shear stress drops to 0.0368 which is less than that of the bare cylinder. The reducton of Reynolds shear stress is approximately 10%.

The right side of Figure 6 illustrates the streamwise velocity contours. For all porosities, the occurrence of reverse flow is observed in the first field of view for all porosities. The location of reverse flow moves upstream with increasing the porosity. For the porosities of β < 0.7, the peak value of negative streamwise velocity is decreased remarkably while the peak value is approximately equal to that of the bare cylinder for the porosity of 0.7

In terms of the turbulent kinetic energy (TKE), the results show similarity with Reynolds shear stress and streamwise velocity component. The peak values of turbulent kinetic energy for bare cylinder and the inner cylinder- outer permeable cylinder arrangement are given in Figure 7. It is obviously seen that for the porosities smaller than β = 0.7, the outer permeable cylinder does not have dramatic effect on the attenuation of vortex shedding downstream of the inner cylinder- outer permeable cylinder arrangement. For these porosities, the peak values of TKE are greater than that of the bare cylinder. For the porosity of β = 0.7, the peak value of TKE decreases to 0.132, less that of the bare cylinder case, as a consequence of suppression of unsteady vortex shedding.

4. Discussion

To represent the effects of the permeable cylinder, the flow structures in the wake region of bare cylinder, permeable cylinder and inner-outer permeable cylinder arrangement were investigated. As the well-known Karman Vortex Street occurs downstream of the bare cylinder, low frequency Karman Vortex Street compared to that of the bare cylinder forms downstream of the permeable cylinder. For the permeable cylinder case, the peak value of Reynolds shear stress diminishes gradually as the porosity value rises and the minimum value of streamwise velocity rises since the momentum transfer from the open area on the surface of the permeable cylinder into the flow behind the permeable cylinder increases as a consequence of enlargement of the open area. Moreover, the location of the minimum value of streamwise velocity immigrates further downstream of the permeable cylinder as the porosity value increases. Additionally, for the porosity of β = 0.7, the concentration of Reynolds shear stress disappears at the centerline of the permeable cylinder along the flow fields while the contours of Reynolds shear stress concentrate in the shear layers due to the effectiveness of Kelvin-Helmholtz vortices. In terms of the inner cylinder-outer permeable cylinder arrangement, the inner and outer permeable cylinders behave like an impermeable cylinder having the diameter of D=45 mm for the porosities of β = 0.4, 0.5 and 0.6. The open area on the surface of the permeable cylinder is too narrow to let the flow in order to penetrate into the wake region. Therefore, the magnitude of Reynolds shear stress increases slightly compared to the bare cylinder case and at the same time, the peak values of TKE are greater than that of the bare cylinder for these

porosities. The reason of this raise of the turbulent kinetic energy is velocity fluctuations downstream of the outer permeable cylinder. Fortunately, the location of peak concentration of TKE moves further away from the base of the outer permeable cylinder with increasing porosity. In addition, since the unsteady flow structure downstream of the inner-outer permeable cylinder arrangement cannot be prevented, the reverse flow appears downstream of the cylinder arrangement as a sign of the existence of stagnation point for all porosities. On the other hand, the permeable cylinder having the porosity of $\beta = 0.7$ has a substantial effect on the control of large-scale vortical structure downstream of the cylinder arrangement.

Furthermore, Gozmen and Akilli [12] indicated that permeable cylinders placed around a solid cylinder are effective on the control of vortex shedding. They investigated the flow around the permeable cylinder for the diameter ratios D/d=1.25, 1.75,2, 2.5 and 3.0. Their study revealed that the diameter ratio of D/d=1.75 attenuates the vortex shedding behind the cylinder arrangement as the ratio of D/d=1.25 is not effective on the attenuation of vortex shedding. The diameter ratio of D/d=3.0 is the most effective one relative to the other diameter ratios. In terms of the porosity values, the maximum reduction in the turbulent statistics is obtained from β=0.7 case. For the β=0.8 and 0.85, the effect of the inner cylinder on the flow structure increases as a result of the increase in the open area of the outer permeable cylinder. Consequently, co-decision of these studies is that there is a critial diameter ratio to control vortex shedding downstream of the inner cylinder- outer permeable cylinder arrangement and this diameter ratio is D/d=1.5.

5. Conclusions

In this study, the control of vortex shedding downstream of a solid cylinder is aimed by concentrically placing a permeable cylinder in deep water. To reveal the effect of permeable cylinder, flow structures downstream of the bare cylinder, permeable cylinder and inner cylinder-outer permeable cylinder arrangement have been investigated. The experiments show that the permeable cylinder is effective on the suppression of vortex shedding in the wake region for all porosities. As the porosity increases, the turbulent intensity of the flow decreases as a consequence of enlargement of the open area. In terms of the inner cylinder-outer permeable cylinder arrangement, it is understood that the inner-outer cylinder arrangement having the diameter ratio of D/d=1.5 is not effective on the attenuation of vortex shedding downstream of the inner cylinder as expected. For the porosities of $\beta = 0.4$, 0.5 and 0.6, the open area on the surface of the permeable cylinder is too narrow to let the flow in order to penetrate into the wake region. The desired effect on the control of wake region is only achieved with the permeable cylinder having the porosity of $\beta = 0.7$. According to this work and the previous study of Gozmen and Akilli [12], it is decided that the diameter ratio of D/d=1.5 in the diameter ratios D/d=1.25, 1.50, 1.75, 2, 2.5 and 3.0 is the critial diameter ratio to suppress vortex shedding downstream of the inner cylinder- outer permeable cylinder arrangement.

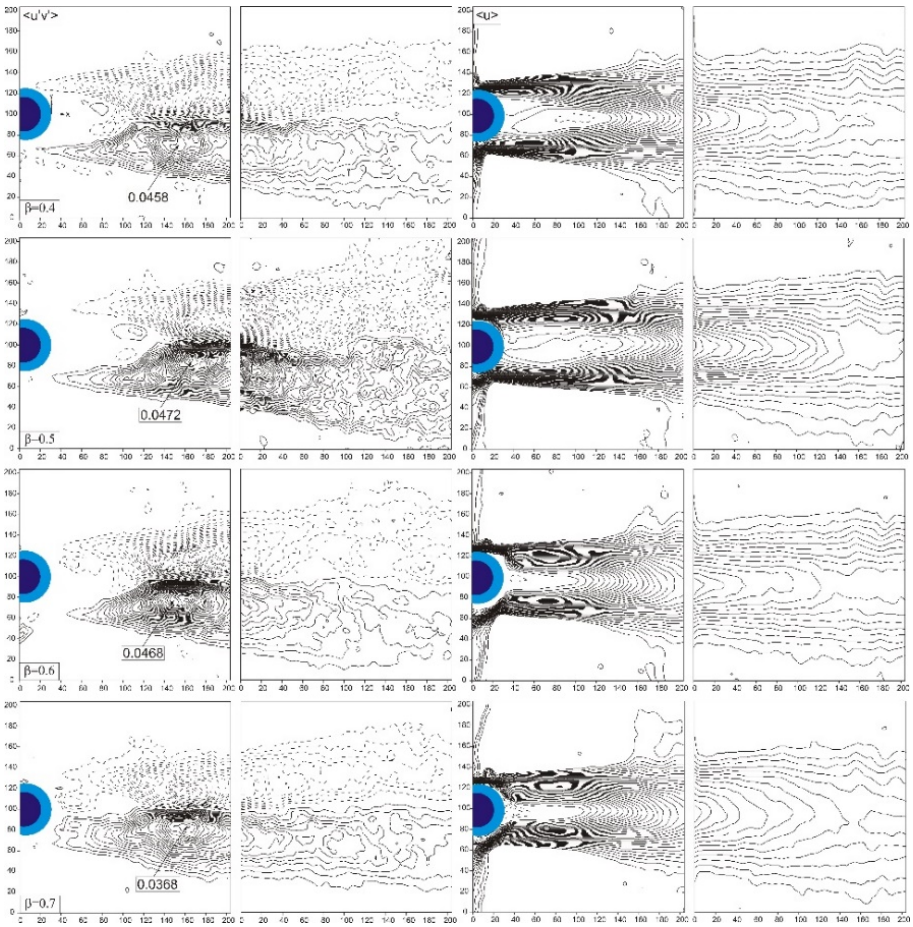

Fig. 6. Contours of normalized Reynolds shear stress and time-averaged streamwise velocity downstream of the inner cylinder- outer permeable cylinder arrangement for all porosity values β of the diameter ratio of D/d=1.5

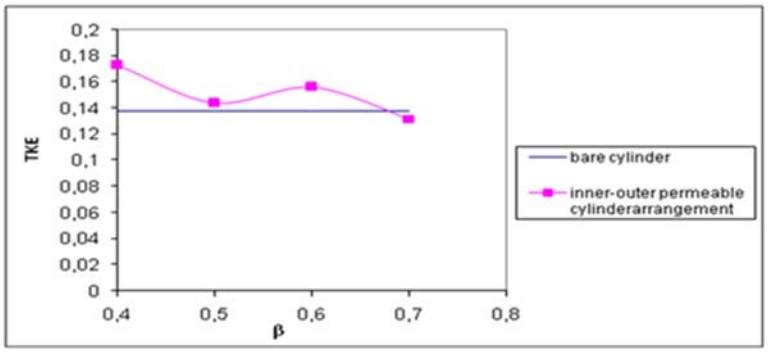

Fig. 7. Peak values of Turbulent Kınetic energy for the bare cylinder and all porosity values β of D/d=1.5

References

[1] Choi H, Jeon WP, Kim J. Control of flow over a bluff body. Annual Review of Fluid Mechanics 2008; 40:113–139. http://dx.doi.org/10.1146/annurev.fluid.39.050905.110149

[2] Strykowski PJ, Sreenivasan KR. On the formation and suppression of vortex shedding at low Reynolds numbers. Journal of Fluid Mechanics 1990; 218:71–107. http://dx.doi.org/10.1017/S0022112090000933

[3] Lee SJ, Lee SI, Park CW. Reducing the drag on a circular cylinder by upstream installation of a small control rod. Fluid Dynamics Research 2004; 34:233-250. http://dx.doi.org/10.1016/j.fluiddyn.2004.01.001

[4] Lim HC and Lee SJ. Flow control of a circular cylinder with O-rings. Fluid Dyn. Res. 2004; 35(2):107-122. http://dx.doi.org/10.1016/j.fluiddyn.2004.05.001

[5] Kwon K, Choi H. Control of laminar vortex shedding behind a circular cylinder using splitter plates. Phys. Fluids 1996; 8:479–486. http://dx.doi.org/10.1063/1.868801

[6] Ozono S. Flow control of vortex shedding by a short splitter plate asymmetrically arranged downstream of a cylinder. Phys. Fluids 1999; 11:2928–2934. http://dx.doi.org/10.1063/1.870151

[7] Akilli H, Sahin B, Tumen NF. Suppression of vortex shedding of circular cylinder in shallow water by a splitter plate. Flow Meas. Instrum. 2005; 16:211–219. http://dx.doi.org/10.1016/j.flowmeasinst.2005.04.004

[8] Gozmen B, Akilli H, Sahin B. Passive control of circular cylinder wake in shallow flow. Measurement 2013; 46(3):1125-1136. http://dx.doi.org/10.1016/j.measurement.2012.11.008

[9] Shukla S, Govardhan RN, Arakeri JH. Dynamics of a flexible splitter plate in the wake of a circular cylinder. Journal of Fluids and Structures 2013; 41:127–134. http://dx.doi.org/10.1016/j.jfluidstructs.2013.03.002

[10] Bruneau CH and Mortazavi I. Control of vortex shedding around a pipe section using a porous sheath. Int. J. Offshore Polar 2006; 16(2):1-7.

[11] Bhattacharyya S, Dhinakaran S and Khalili A. Fluid motion around and through a porous cylinder. Chem. Eng. Sci. 2006; 61(13):4451-4461 http://dx.doi.org/10.1016/j.ces.2006.02.012

[12] Gozmen B and Akilli H. Flow control downstream of a circular cylinder by a permeable cylinder in deep water. Wind and Structures 2014; 19(4):389-404 http://dx.doi.org/10.12989/was.2014.19.4.389

[13] Sobera, M.P., Kleijn, C.R. and Van den Akker, H.E.A. (2006), "Subcritical flow past a circular cylinder surrounded by a porous layer", Phys. Fluids, 18(3), 038106. http://dx.doi.org/10.1063/1.2189284

[14] Doll, S.S., Kopp, G.A. and Martinuzzi, R.J. (2008), "The suppression of periodic vortex shedding from a rotating circular cylinder", J. Wind Eng. Ind. Aerod., 96(6-7), 1164-1184. http://dx.doi.org/10.1016/j.jweia.2007.06.038

[15] Fransson, J.H.M., Konieczny, P. and Alfredsson, P.H. (2004), "Flow around a porous cylinder subject to continuous suction or blowing", J. Fluid Struct., 19(8), 1031-1048. http://dx.doi.org/10.1016/j.jfluidstructs.2004.06.005

[16] Li, Z., Navon, I.M., Hussaini, M.Y. and Le Dimet, F.X. (2003), "Optimal control of cylinder wakes via suction and blowing", Comput. Fluids, 32(2), 149-171. http://dx.doi.org/10.1016/S0045-7930(02)00007-5

[17] Akansu, Y.E. and Fırat, E. (2010), "Control of flow around a square prism by slot jet injection from the rear surface", Exp. Therm. Fluid Sci., 34(7), 906-914. http://dx.doi.org/10.1016/j.expthermflusci.2010.02.007

[18] Cattafesta, L.N., Garg, S. and Shukla, D. (2001), "Development of piezoelectric actuators for active flow control", AIAA J., 39(8), 1562-1568. http://dx.doi.org/10.2514/2.1481

[19] M. Raffel, C.E. Willert, J. Kompenhans, Particle Image Velocimetry a Practical Guide,

Springer, Göttingen, 1998. http://dx.doi.org/10.1007/978-3-662-03637-2
[20] Ozkan, G.M., Oruc, V., Akilli, H. and Sahin, B. (2012), "Flow around a cylinder surrounded by a permeable cylinder in shallow water", Exp. Fluids, 53(6), 1751-1763. http://dx.doi.org/10.1007/s00348-012-1393-2
[21] Pınar E., Ozkan G.M., Durhasan T., Akıllı H., Sahin B. (2015), "Flow structure around perforated cylinders in shallow water", Journal of Fluids and Structures 55, 52–63. http://dx.doi.org/10.1016/j.jfluidstructs.2015.01.017

[22] M. Bovand a, S. Rashidi a,n, M. Dehghan b, J.A. Esfahani a, M.S. Valipour (2015), Control of wake and vortex shedding behind a porous circular obstacle by exerting an external magnetic field, Journal of Magnetism and Magnetic Materials 385, 198–206. http://dx.doi.org/10.1016/j.jmmm.2015.03.012
[23] Feng LH, Wang JJ (2010) Circular cylinder vortex-synchronization control with a synthetic jet positioned at the rear stagnation point. J Fluid Mech 662:232–259. http://dx.doi.org/10.1017/S0022112010003174